HHS Public Access

Author manuscript

Proc SPIE Int Soc Opt Eng. Author manuscript; available in PMC 2015 June 23.

Published in final edited form as:

Proc SPIE Int Soc Opt Eng. 2008 January 19; 6845: . doi:10.1117/12.763806.

Integrated light dosimetry system for prostate photodynamic therapy

Jun Li[*], **Timothy C. Zhu**, **Xiaodong Zhou**, **Dimofte Andreea**, and **Jarod C. Finlay**

Department of Radiation Oncology, University of Pennsylvania, Philadelphia, PA 19104

Abstract

A light dosimetry system is developed for prostate PDT, which integrates four main components: a light fluence rate calculation engine, an optimization tool for treatment planning, a light delivery system, and an *in vivo* light fluence rate measurement system. Three-dimensional light fluence rate distribution in a prostate is calculated using a kernel algorithm, which takes into account of heterogeneous optical properties. A Cimmino optimization algorithm is used to optimize the parameters of the cylindrical diffusing fibers (CDFs) to generate uniform PDT dose (or light fluence rate under uniform drug distribution) to cover the heterogeneous prostate. The light delivery system is composed of a 12-channel beamsplitter and the intensities of each channel (i.e., source) are controlled individually by programmable motorized attenuators. Our tests show that the light fluence rate calculation is fast and the accuracy is close to that of a finite-element method model, and the approach that uses the treatment CDFs to determine optical properties, improves the accuracy of light fluence rate prediction. The light delivery system allows real time control of the light source intensities for both PDT dosimetry and PDT light delivery. Integrating the fast light fluence rate calculation, optimization, instant source intensity adjustment, and *in vivo* light fluence rate measurement, the dosimetry system is suitable for prostate PDT.

Keywords

photodynamic therapy; light dosimetry; light fluence rate; heterogeneity; kernel method; optimization; light delivery; prostate

1. INTRODUCTION

Photodynamic therapy (PDT)[1] is a treatment modality employing light of certain wavelength in the presence of oxygen to activate a photosensitizer which then causes localized cell death or tissue necrosis. The efficacy of PDT depends upon multiple factors including light fluence, photosensitizer concentration, and tissue oxygen level.[2]

Currently interstitial light delivery is an efficient illumination scheme for prostate PDT, whereby optical fibers are placed directly into the bulky tumors or organs. We have initiated a protocol for motexafin lutetium (MLu)-mediated PDT of the prostate in patients at the University of Pennsylvania.[3–6] In the prostate PDT, laser at wavelength of 732 nm was used

[*]Current address: Department of Radiation Oncology, Thomas Jefferson University, Philadelphia, PA 19107. Jun.Li@jefferson.edu

to activate MLu. Cylindrical diffusing optical fibers (CDFs) with active lengths between 1 and 5 cm were used as light sources. Catheters were inserted in parallel into the prostate with the guidance of an ultrasound unit and a template. The CDFs were placed in the catheters, which had lengths larger than the prostate size to ensure that the prostate was completely covered during treatment.

Light fluence delivered to the tumor volume is an important dosimetry quantity in PDT. Light delivery in prostate PDT faces the challenge of optical heterogeneity. In this study, we developed a light dosimetry system, with the effort to deliver accurate light fluence to a heterogeneous prostate. The system has four main components (Fig. 1): a three-dimensional (3D) light fluence rate calculation system, a light source optimization system, a light delivery system, and an *in-vivo* light fluence rate measurement system. The former two systems, together with a transrectal ultrasound (TRUS) image acquisition system, compose a treatment planning system. The *in-vivo* light fluence rate measurement system measures light fluence rate in real-time during PDT, which monitors the light delivery and checks the light fluence rate calculation. Optical heterogeneity is taken into account in the light fluence rate calculation and the light source optimization. The light intensity delivered to each CDF can be adjusted individually with computer-controlled attenuators.

2. METHOD

2.1 *In-vivo* light fluence rate measurement

Figure 2 shows a typical arrangement of light sources and detectors in a prostate PDT. In the treatment, a prostate is divided into four regions (quadrants): right upper quadrant (RUQ), left upper quadrant (LUQ), right lower quadrant (RLQ), and left lower quadrant (LLQ). Light fluence rates are measured in the center of each quadrant. An isotropic detector is scanned parallel to the CDFs and light fluence rates are measured during the treatment. Figure 3 shows light fluence rates measured in a quadrant of a patient prostate. Measured light fluence rates are used to examine the heterogeneous kernel model calculation.

2.2 3D light fluence rate calculation

Light fluence rate calculation is based on the diffusion equation describing light transport in biological tissue,[7]

$$-\nabla \cdot (D(\mathbf{r})\nabla\phi)+\mu_a(\mathbf{r})\phi=S \quad (1)$$

where the diffusion coefficient $D=1/3\mu_s'$ (μ_s' is the reduced scattering coefficient), μ_a is the absorption coefficient, and S is the source power (in units of mW or W). For heterogeneous medium, i.e., when D and μ_a are spatially dependent, Eq. 1 can only be solved numerically.

We had developed a finite-element method (FEM) model to calculate light fluence rate distribution in prostate.[7] The FEM model calculation, which takes ~300 seconds, is not fast enough for real-time treatment planning. In order to perform real-time treatment planning, we have developed a heterogeneous kernel model, which takes about 1/3 of the time of the FEM model calculation. Optical heterogeneity is taken into account in the calculation. The

kernel model is based on the assumption of spherical shell distribution of optical properties. Light fluence rate in the *i*th shell ($r_{i-1}<r<r_i$) is expressed as[8]

$$\phi_i = C\left(\frac{p_i \mu_{s,i}'}{4\pi r} e^{-\mu_{eff,i} r} + \frac{q_i \mu_{s,i}'}{4\pi r} e^{\mu_{eff,i} r}\right), \quad (r_{i-1}<r<r_i) \quad (2)$$

where C, p_i, and q_i are coefficients determined by optical properties, and $\mu_{s,i}'$ and $\mu_{eff,i}(r)$ are reduced scattering coefficient and effective attenuation coefficient in the *i*th shell, respectively.

2.3 Light source optimization

With light fluence rates obtained using the heterogeneous kernel model calculation, the Cimmino algorithm[9] is applied to optimize source strengths in a heterogeneous prostate. The optimization is to find individual source strengths that collectively deliver a prescribed dose to the (target) prostate without exceeding specified maximum dose values for the target and non-target regions (urethra, rectum, and unspecified background), when given all the source locations and source lengths.

The discretized simple inverse problem can be written as

$$b_i^{\min} \le \sum_j A_{ij} x_j \le b_i^{\max} \quad (i=1,\ldots,I; j=1,\ldots,J) \quad (3)$$

or in matrix form as

$$\mathbf{b}^{\min} \le \mathbf{A}\mathbf{x} \le \mathbf{b}^{\max} \quad (4)$$

where I is the number of voxels (or constraint points); $\mathbf{b}^{\max}$ and $\mathbf{b}^{\min}$ are the dose bounds on the voxels; J is the number of light sources; a component of matrix **A** denoted A_{ij} gives the dose absorbed at voxel i per unit strength of light source j. A positive lower bound prescribes a minimum dose for a prostate (target) voxel; it is zero for non-prostate voxels. An upper bound on dose is provided for every voxel. The goal is to find the vector **x** of source strengths that satisfies the inequality constraints of the expression (4). The matrix **A** is a 2-D light fluence table for sources of all allowed lengths, which is calculated with the heterogeneous kernel model. Optical heterogeneity is taken into account in the optimization.

2.4 Treatment planning system

The light fluence rate calculation system, the light source optimization system, and a TRUS image acquisition system, compose the treatment planning system. Figure 4 shows a picture of the treatment planning system, which is connected to a TRUS unit during a treatment. Figure 5 shows the diagram of the treatment planning system. In a treatment, TRUS images are acquired from a TRUS unit with an image grabber (DT 3120, Data Translation, Inc.). The images are digitized and the contours of the prostate are used for 3D volume reconstruction. The measured source and detector locations are used in the light fluence rate

calculation, where the heterogeneous kernel model is applied. The calculated light fluence rates are used in light source optimization. Optical properties are needed as input in the light fluence rate calculation.

2.5 Optical property measurement using treatment linear source

In our previous study, a point source was used in the optical property measurement (Fig. 6(a)).[3] An isotropic detector was scanned to measure light fluence rates generated by the point source and optical properties were obtained by fitting the light fluence rate distributions. Usually the optical property measurement was made at a few source locations to obtain 3D optical properties, which was slow and was not suitable for real-time treatment planning. To perform real-time treatment planning, we have developed a technique, which uses treatment linear sources instead of point sources to measure optical properties directly (Fig. 6(b)).[10] The measurement takes much less time to obtain optical properties than the point source measurement. For instance, the point source measurement needs 8 scans whereas the linear source measurement needs only 1 scan. The technique was examined by using the obtained optical properties to predict light fluence rates in the treatment and comparing the calculation with measurements.

2.6 Light delivery

Figure 7 shows the diagram of the light delivery system. The laser beam from a diode laser of 732 nm is delivered to a 12-channel beam splitter through an optic fiber. The split beams are sent to individual attenuators. The transmission of each attenuator can be adjusted with a step motor, which is controlled by a computer. Different light powers are sent to each cylindrical diffusing fiber to deliver uniform light fluence to cover the prostate. The system has 16 attenuators, which can be used for 16 CDFs. Figure 8 shows a picture of a prostate phantom in an experiment. Laser was delivered to the phantom through the beam splitter, 12 attenuators, and 12 CDFs.

3. RESULTS AND DISCUSSION

Figure 9 shows the comparison of light fluence rates obtained with the heterogeneous kernel model, a FEM model, and measurements. The results show that with known optical properties, the heterogeneous kernel model can predict light fluence rates close to those of the FEM calculation and measurements.

Figure 10(a) and (b) show isodose lines (100 J/cm^2) generated by 12 sources in a patient prostate, which were obtained with uniform source weights and Cimmino optimized source weights, respectively. Optical heterogeneity was observed in the patient: absorption was significant in the upper region of the prostate. The dose generated by the 12 sources with uniform source weights does not cover the upper region. When the Cimmino optimization is applied, the dose coverage is improved (Fig. 10(b)). However, because the region is highly opaque and light penetration is limited, the improvement is limited. If more sources are used, the prostate can be well covered with a Cimmino optimized plan (Fig. 10(c)). The Cimmino optimized plan, which uses more sources in the opaque region, improves the

coverage of the prostate remarkably. The results demonstrate that the Cimmno optimization can be applied to improve dose coverage in a heterogeneous prostate.

Figure 11 shows the graphic user interface of the treatment planning system during a prostate phantom experiment. TRUS images were acquired into the system, the prostate phantom was contoured (magenta line), and source locations and detector locations were digitized, which were indicated with yellow circles and red “x” markers, respectively. An isodose line of 150 J/cm^2 was shown in red line.

The optical property measurement using treatment linear sources was examined by comparing light fluence rates calculated using the optical properties with those measured in the treatment. Figure 12 shows the comparison of the light fluence rates in a prostate phantom, which shows good agreement between the calculation and measurement. The use of treatment linear source to measure optical properties for light fluence rate calculation reduces the measurement time. The source location errors in point source measurement are avoided and the accuracy of light fluence rate predication is improved. The technique is promising for real-time treatment planning.

4. CONCLUSIONS

Optical heterogeneity has been taken into account in the calculation of light fluence rate distribution and the light source optimization in prostate PDT. The study shows that the optical property measurement using treatment linear source is promising for real-time treatment planning. Integrated with the TRUS image acquisition, 3D light fluence rate calculation, source optimization, *in vivo* light fluence rate measurement providing feedback, and computer controlled light delivery, the light dosimetry system is suitable for prostate PDT. Further tests of the system are expected in future studies.

Acknowledgments

This work is supported by grants from Department of Defense (DOD) DAMD17-03-1-0132 and National Institute of Health (NIH) R01 CA109456.

References

1. Dougherty TJ, Gomer CJ, Henderson BW, Jori G, Kessel D, Korbelik M, Moan J, Peng Q. Photodynamic therapy. J Natl Cancer Inst. 1998; 90:889–905. [PubMed: 9637138]
2. Wilson BC, Patterson MS, Lilge L. Implicit and explicit dosimetry in photodynamic therapy: a new paradigm. Lasers Med Sci. 1997; 12:182–199. [PubMed: 20803326]
3. Zhu TC, Dimofte A, Finlay JC, Stripp D, Busch T, Miles J, Whittington R, Malkowicz SB, Tochner Z, Glatstein E, Hahn SM. Optical properties of Human Prostate at 732nm measured in vivo during motexafin lutetium-mediated photodynamic therapy. Photochem photobiol. 2005; 81:96–105. [PubMed: 15535736]
4. Zhu TC, Finlay JC, Hahn SM. Determination of the Distribution of Light, Optical Properties, Drug Concentration, and Tissue Oxygenation *in-vivo* in Human Prostate during Motexafin Lutetium-Mediated Photodynamic Therapy. J Photochem Photobiol B: Biol. 2005; 79:231–241.
5. Zhu, TC.; Li, J.; Finlay, JC.; Dimofte, A.; Stripp, D.; Malkowicz, BS.; Hahn, SM. *In-vivo* light dosimetry of interstitial PDT of human prostate. Proceedings of SPIE; San Jose, CA. 2006. p. 61390L

6. Zhu TC, Finlay JC. Prostate PDT dosimetry. Photodiagnosis and Photodynamic Therapy. 2006; 4:234–246. [PubMed: 25046988]
7. Li, J.; Zhu, TC.; Finlay, JC. Study of light fluence rate distribution in photodynamic therapy using finite-element method. Proceedings of SPIE; San Jose, CA. 2006. p. 61390M
8. Li, J.; Zhu, TC. Modeling light fluence rate distribution in optically heterogeneous prostate photodynamic therapy using a kernel method. Proceedings of SPIE; San Jose, CA. 2007. p. 64270M
9. Altschuler MD, Zhu TC, Li J, Hahn SM. Optimized interstitial PDT prostate treatment planning with the Cimmino feasibility algorithm. Med Phys. 2005; 32(12):3524–3536. [PubMed: 16475751]
10. Dimofte, A.; Finlay, JC.; Li, J.; Zhu, TC. Determination of optical properties in a heterogeneous turbid media using a cylindrical diffusing fiber. Proceedings of SPIE; San Jose, CA. 2008. (to be published)

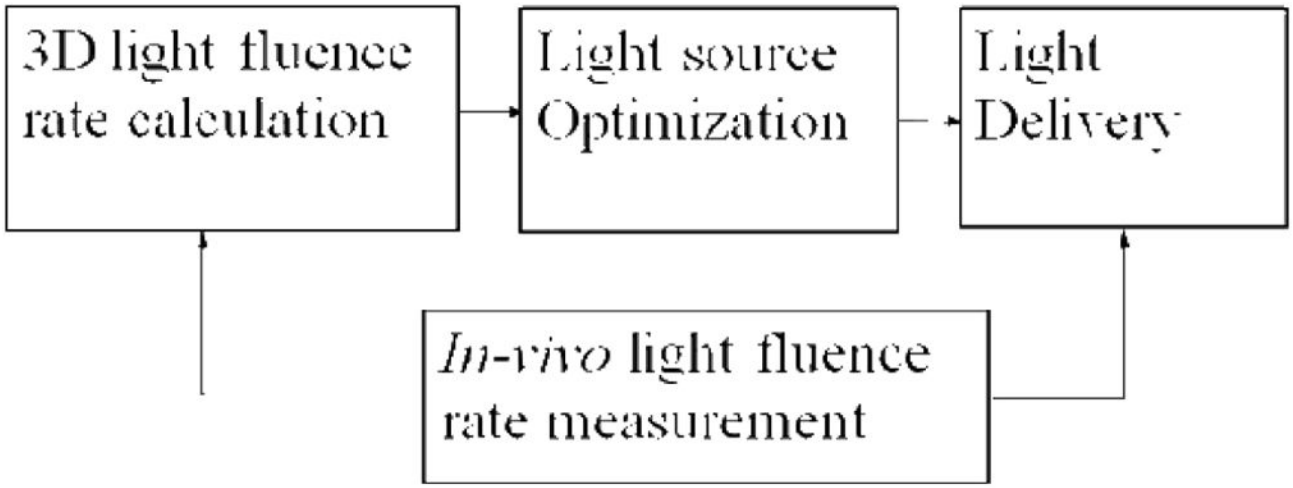

Figure 1.
Diagram of the integrated light dosimetry system.

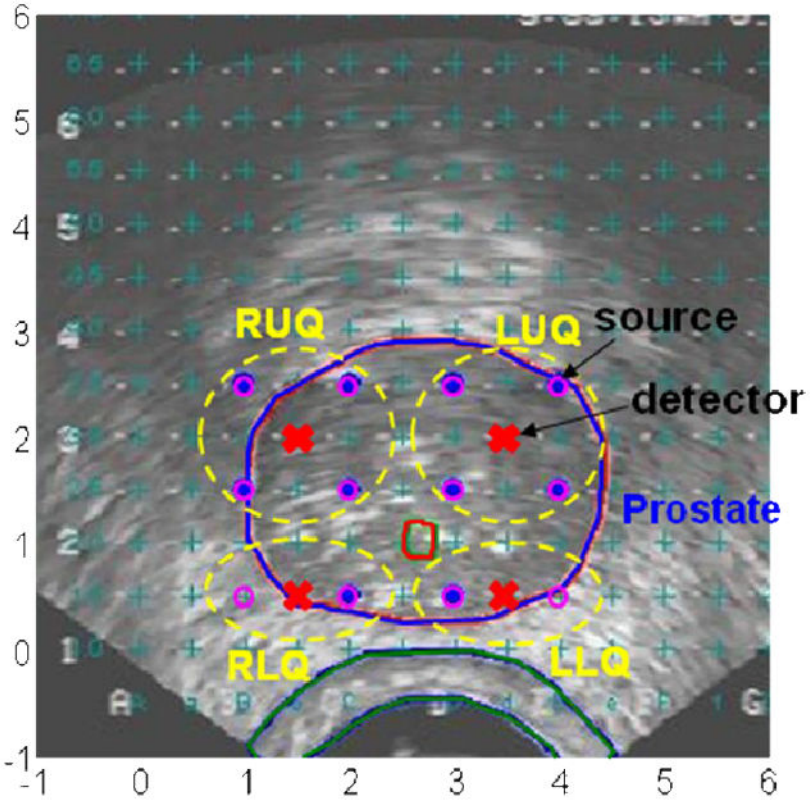

Figure 2.
A typical arrangement of sources and detectors in prostate PDT.

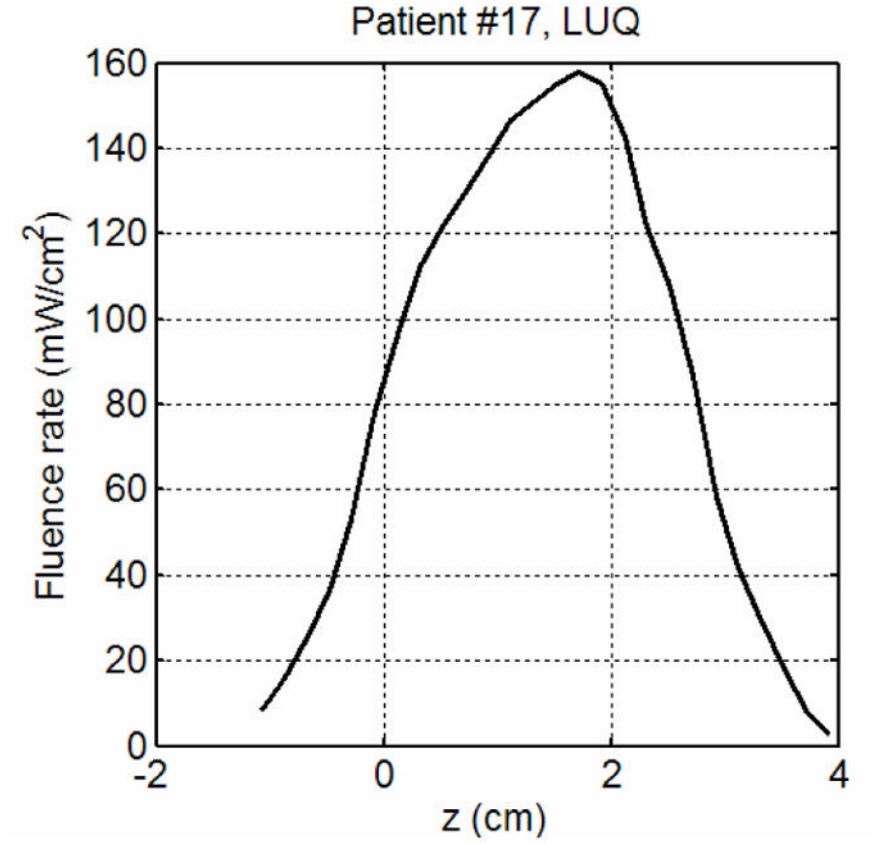

Figure 3.
Light fluence rates measured in a patient.

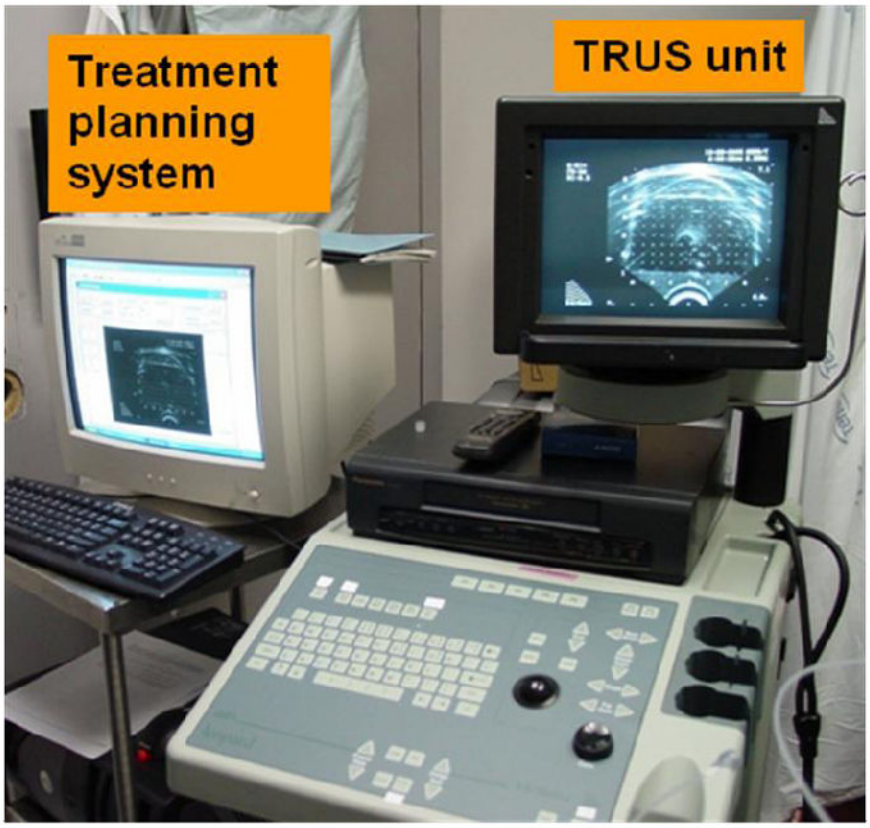

Figure 4.
The treatment planning system (left), which is connected to a transrectal ultrasound (TRUS) unit.

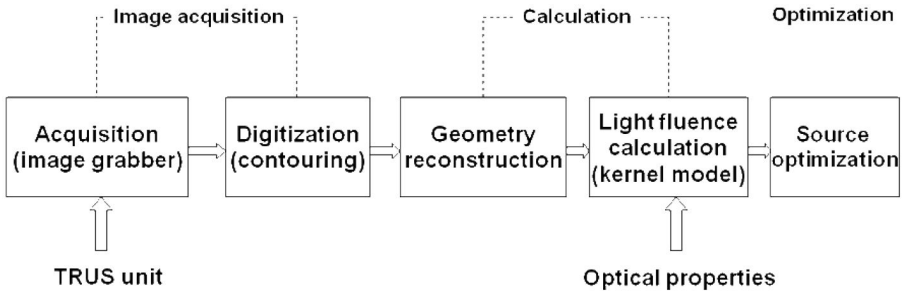

Figure 5.
Diagram of the treatment planning sytem.

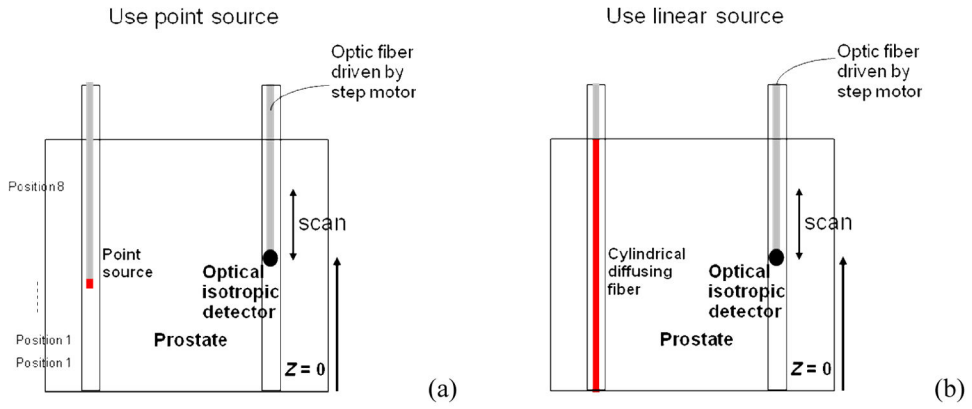

Figure 6.
Optical property measurement using (a) point source, and (b) linear source.

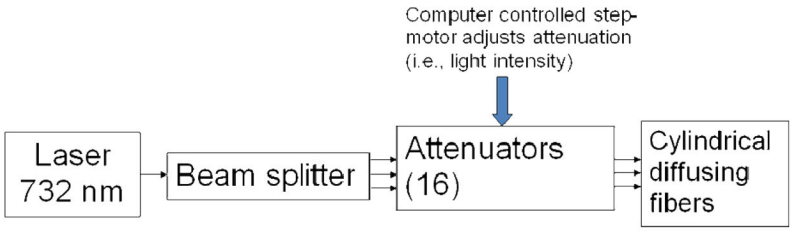

Figure 7.
Diagram of the light delivery system.

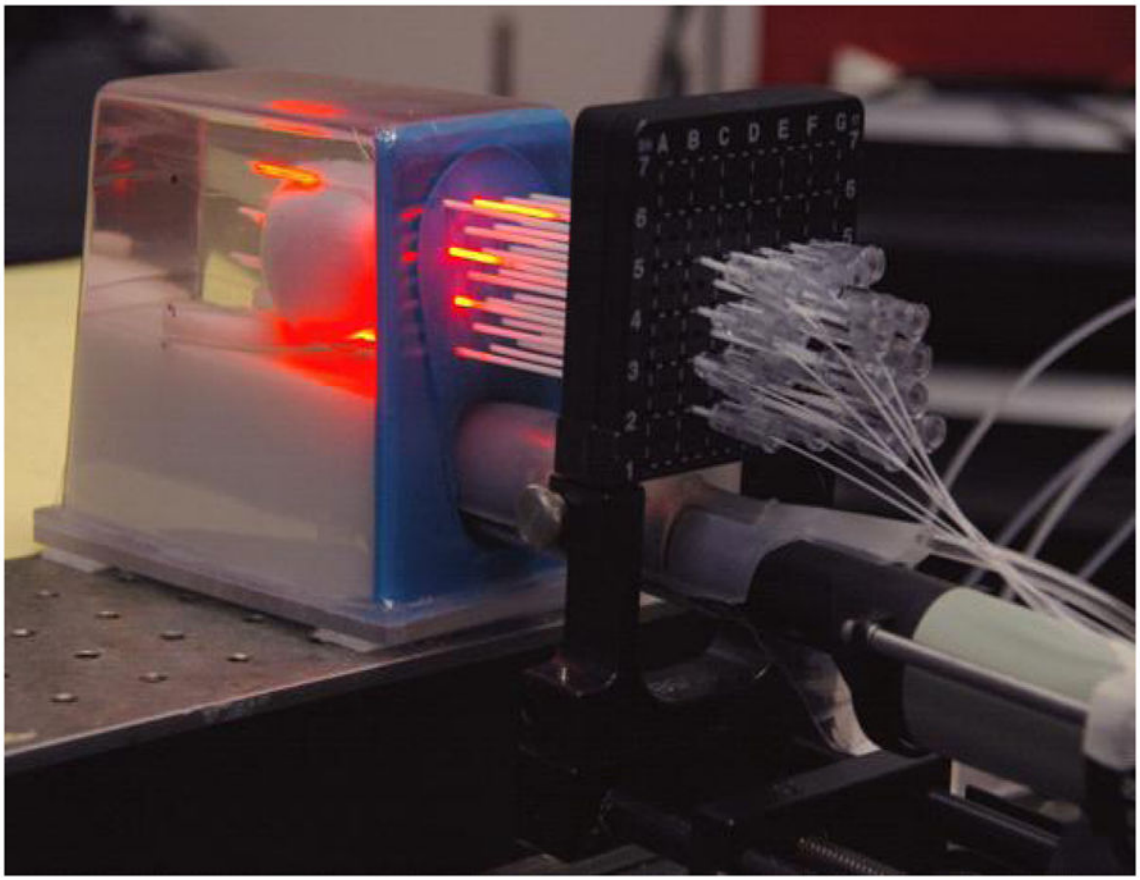

Figure 8.
Picture of a prostate phantom in an experiment. Laser was delivered to the phantom with the beam splitter, attenuators and 12 CDFs.

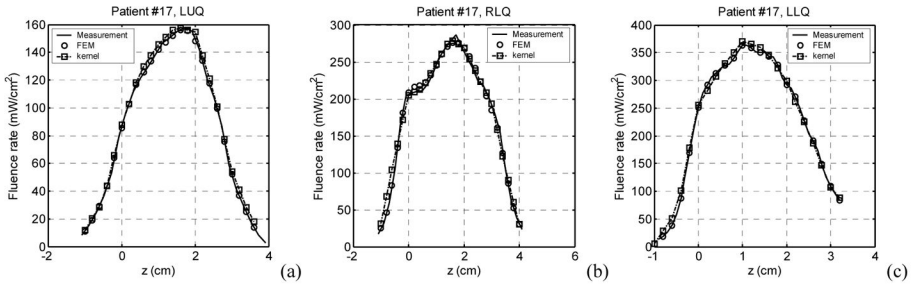

Figure 9.

Comparison of light fluence rates obtained with the heterogeneous kernel model calculation, a FEM model calculation, and measurements, in a patient prostate. (a) LUQ, (b) RLQ, and (c) LLQ.

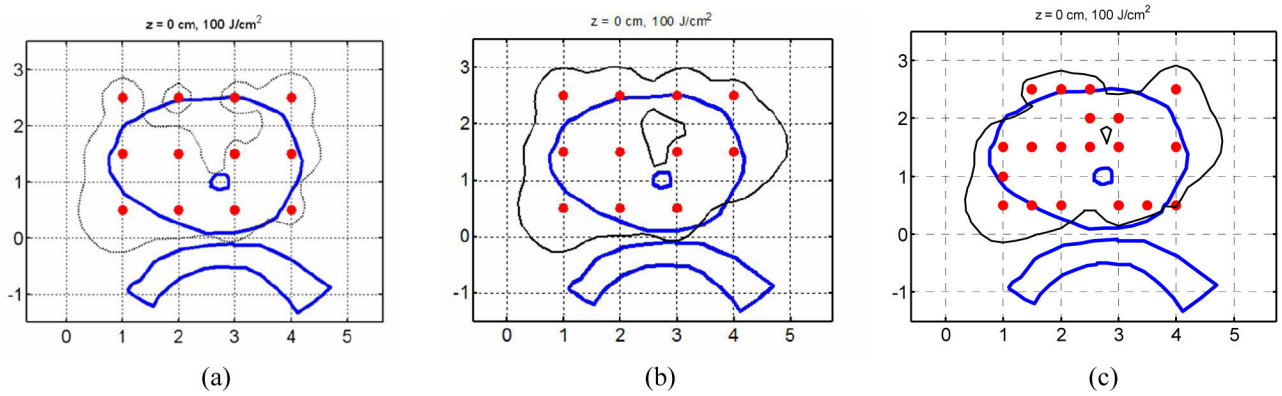

Figure 10.

Comparison of light fluence distributions (the isodose lines are indicated with the black thin lines). (a) 12 sources, uniform source weights; (b) 12 sources, Cimmino optimized source weights; and (c) More than 12 sources, Cimmino optimized source weights. The blue thick lines indicate organs (prostate, urethra, and rectum), and the red dots indicate source locations.

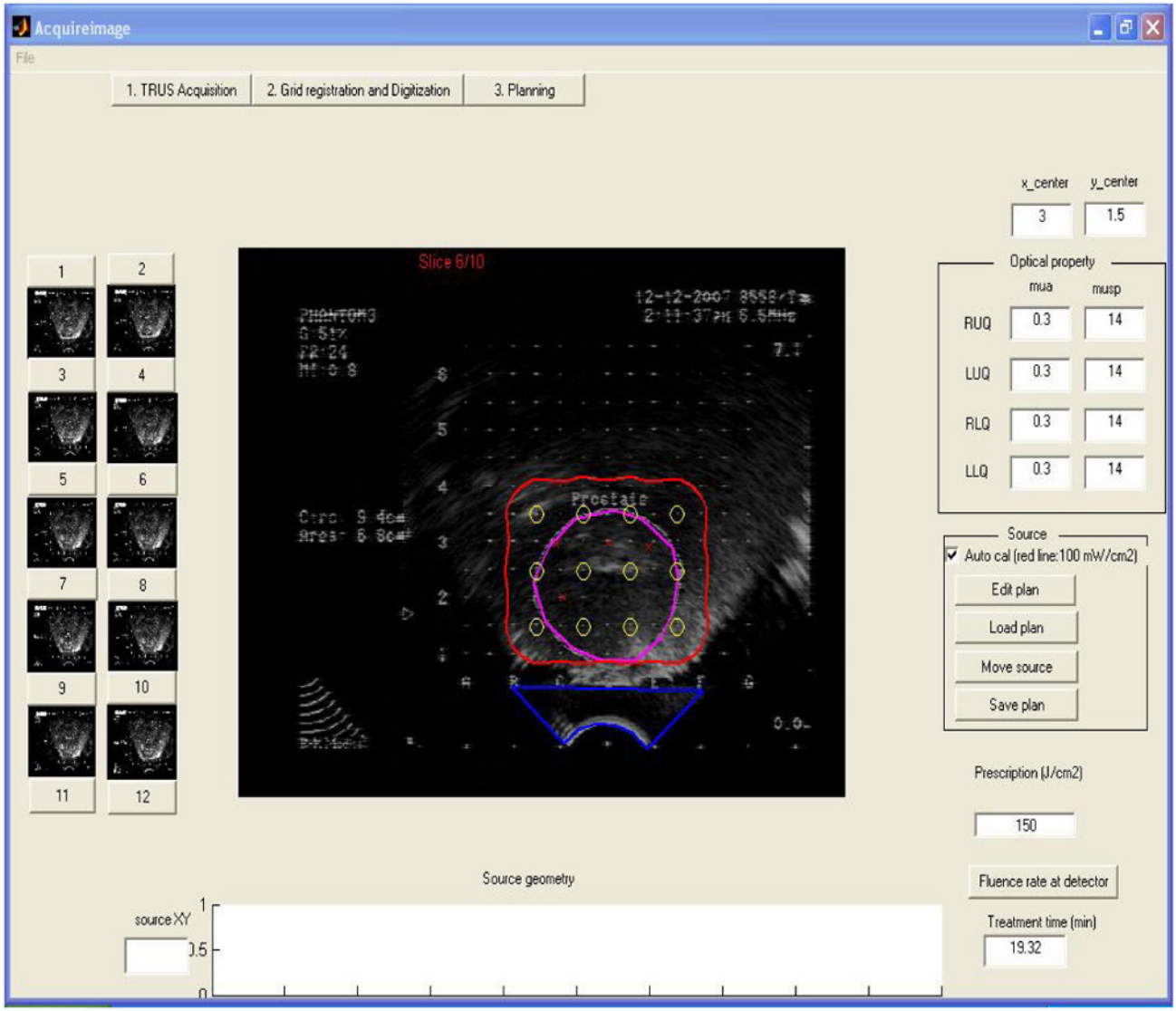

Figure 11.
Graphic user interface of the treatment planning system.

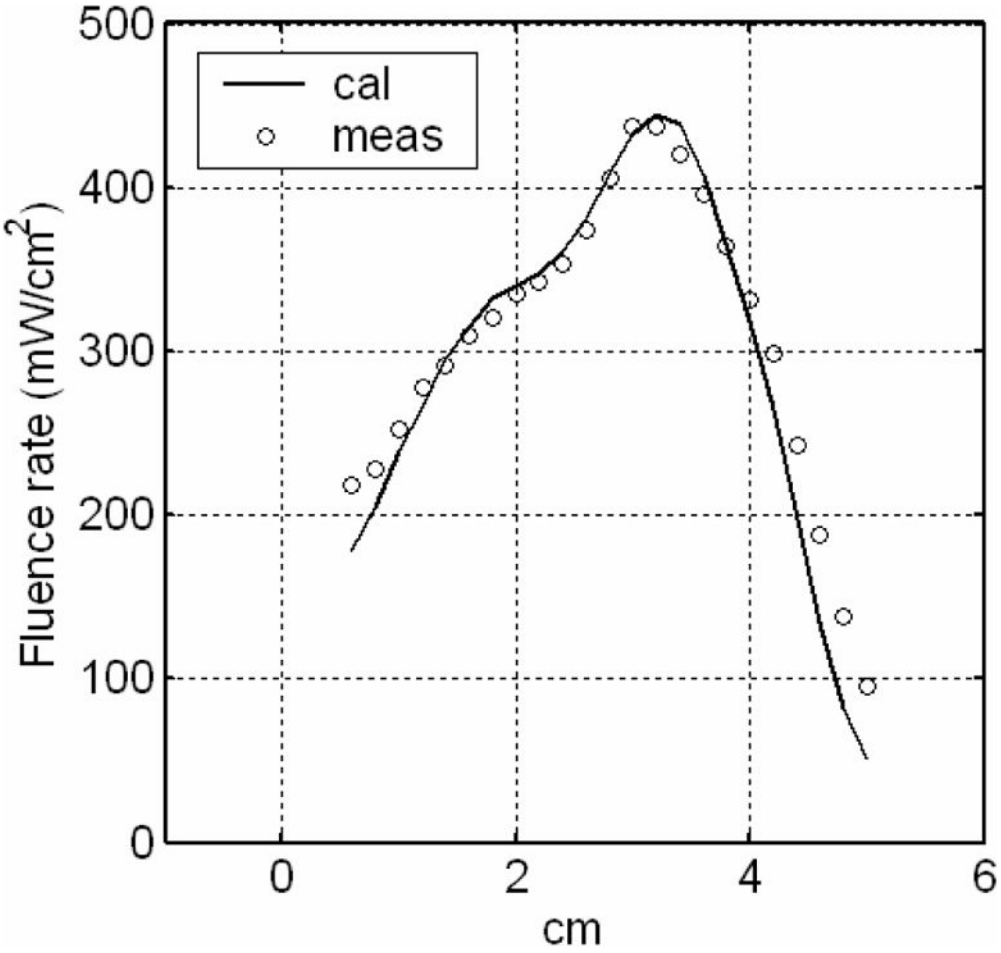

Figure 12.

Examination of the optical property measurement using linear sources. The light fluence rate calculated using the optical properties, which were obtained with the linear source measurement, was compared with the measurement.